IEEE Sensors Letters Volume X(X) (2024)
Chemical and biological sensor

Label-free Electrochemical Immunosensor for Monitoring Kidney Transplant Rejection with Electroactive Antibiofouling Hydrogel

Rohit Gupta[1,2,#,*], Nikolaos Salaris[1,2,#], Ashish Kalkal[1,2,#], Priya Mandal[1,2], Stavroula Balabani[2,3], Reza Motallebzadeh[4], Manish K Tiwari[1,2]

[1] *Nanoengineered Systems Laboratory, Department of Mechanical Engineering, University College London, London, WC1E 7JE, UK*
[2] *Wellcome/EPSRC Centre for Interventional and Surgical Sciences, University College London, London, W1W 7TS, UK*
[3] *FluME, Department of Mechanical Engineering, University College London, London WC1E 7JE, UK*
[4] *Department of Surgery, University College London, Royal Free Campus, London, NW3 2PF, UK*
** Member, IEEE*

Received 6 Mar 2024, revised XX, accepted XX, published XX, current version XX.

Abstract— Diagnosing acute rejection of kidney transplant remains challenging as standard practice relies on monitoring serum creatinine levels and performing biopsies. The former lacks sensitivity, while the latter is invasive. Monitoring Chemokine IP-10 (or CXCL10) in patient samples has shown promising results in addressing these bottlenecks but is measured with expensive and time-consuming protocols such as enzyme-linked immunosorbent assay (ELISA). This does not allow for an individualized approach. The present work describes the development of a novel screen-printed electrode-based electrochemical biosensor for IP-10 detection using an electroactive anti-biofouling hydrogel. The electrode coating is based on glutaraldehyde (GA)-crosslinked 3D nanostructured bovine serum albumin (BSA) hydrogel, whose pores are filled with a highly conductive $Ti_3C_2T_x$ MXene. The formulation is water-based and avoids the use of toxic solvents. The crosslinking mechanism, anti-biofouling characteristics, and electroactivity were characterized by UV-VIS spectroscopy, contact angle measurement, and cyclic voltammetry tests, respectively. The antibody-functionalized MXene/BSA/GA nanocomposite-based sensor allows the detection of IP-10 spiked in human serum by achieving an LOD of 3.3 pg/ml with a linear range across 1-200 pg/ml and a response time of 30 min. The study paves the way toward developing a highly specific multiplexed chemokine profiling platform for point-of-care diagnostics applications to monitor kidney transplant rejection.

Index Terms—Electrochemical Biosensor, Antibiofouling, Kidney Transplant Rejection, Nanocomposite

I. INTRODUCTION

End-stage renal disease affects millions of people globally and kidney transplantation is the optimal treatment option. However, about 10-20% of transplant recipients experience acute rejection (AR) which can lead to a shortened lifespan of the transplanted kidney. This increases the risk of death from cardiovascular disease and cancer.

AR is diagnosed by monitoring serum creatinine (sCr) levels and is confirmed via biopsy. Nevertheless, biopsies are invasive and pose significant risks, and it is often the case that AR persists before a rise in sCr levels is detected [1]. This can cause substantial injuries to the allograft. Therefore, alternative diagnostic tools are necessary to circumvent or optimize biopsy allocation and monitor the efficacy of anti-rejection therapies more effectively.

Chemokines IP-9 (or CXCL9) and IP-10 (or CXCL10) have shown great promise in identifying transplant recipients with AR at an earlier stage [2] and reducing biopsies [3]. Yet, current chemokine measurements rely on enzyme-linked immunosorbent assays (ELISA), which are expensive, have long turnaround times and require high sample volume (10^2-10^3 µl). This does not allow for the timely administration of immunosuppression or anti-rejection therapies based on individual levels of biomarkers.

Affinity-based electrochemical biosensors (EBs) are promising alternatives to detect biomarkers for monitoring AR. EBs offer several benefits such as high sensitivity and specificity, cost-effectiveness, swift sample-to-result turnaround (<30 mins), and minimal sample volume requirement (<10 µL). In addition, these sensors can be seamlessly integrated with a fully automated multiplexed sensing platform for point-of-care (POC) diagnostics applications. However, the choice of suitable material for the sensor surface remains an open question and has received significant attention over the past decade. The sensing surface should offer high interfacial electrical conductivity with ease of antibody functionalization. Another important property of the sensing material is to resist non-specific protein adsorption [4]. EBs are challenged with complex biological fluids (e.g., whole blood, serum, or urine), which contain a plethora of high molecular weight proteins (e.g., albumin). These proteins non-specifically adsorb onto the electrode surfaces, thus passivating the sensor response and diminishing the sensitivity, which was one of the bottlenecks for prior antibody-based EBs for IP-10 sensing [5].

In recent years, bovine serum albumin (BSA)-based crosslinked 3D nanostructured hydrogel has emerged as a promising porous anti-

Corresponding authors: M. K. Tiwari (m.tiwari@ucl.ac.uk) and R. Gupta (rohit.gupta@ucl.ac.uk). #RG, NS, and AK contributed equally.

Digital Object Identifier: 10.1109/LSEN.XXXX.XXXXXXX

biofouling coating that simultaneously reduced non-specific protein adsorption and offered ease of antibody functionalization [6]. However, the crosslinked BSA matrix has poor electrical conductivity, thus hindering charger transfer across the electrode and the bulk electrolyte. This drawback has been addressed by introducing electroactive nanomaterials (e.g., gold nanowires [6], carbon nanotube, reduced graphene oxide [7, 8]) within the pores of the BSA matrix. These electroconductive hydrogels provided ultrasensitive detection of a range of biomarkers while retaining their anti-biofouling characteristics over a long period (up to 1 month).

Titanium carbide ($Ti_3C_2T_x$) MXene has gained attention as a promising 2D material due to its higher electrical conductivity, areal capacitance, and structural integrity [9]. Moreover, MXene has better hydrophilicity (thus higher anti-biofouling ability) than graphene-based materials, making it a suitable candidate as a filler material for the cross-linked hydrogel. Nevertheless, examples of crosslinked BSA hydrogels incorporating MXene as an interfacial material for EBs are sparse [10], especially in the context of developing affinity-based biosensors for AR monitoring.

With this motivation, we develop biofouling-resistant EBs that uses glutaraldehyde (GA)-crosslinked BSA with MXene as a filler material (referred to as MXene/BSA/GA) for rapid sensing of IP-10 spiked in human serum to monitor kidney transplant rejection. A screen-printed carbon electrode (SPCE) chip is modified with the MXene/BSA/GA nanocomposite, which upon antibody functionalization, specifically detects a minimum of 3.3 pg/ml IP-10 with a linear range of 1-200 pg/ml. The EB protocol also benefits from being a single-step procedure, with a nominal response time of ~30 minutes.

II. EXPERIMENTAL METHODS

A. Materials

Delaminated $Ti_3C_2T_x$ MXene nanoflakes were procured from Nanoplexus Ltd. SPCE chips (DropSens 110) integrated with three electrodes was purchased from Metrohm Ltd (working electrode (WE): carbon, counter electrode (CE): carbon, and reference electrode (RE): silver) (Fig. 1A). Hexaaminеruthenium(III) chloride and potassium chloride were supplied by Chemlab Ltd. Phosphate buffer saline (PBS) tablets, human anti-IP-10 antibody (CHC2363), human IP-10 protein (CHC2363), 2-(N-morpholino)ethanesulfonic acid (MES), N-hydroxysuccinimide (NHS), and human AB serum were purchased from Thermo Fisher. Bovine serum albumin (BSA), 70% GA, *N*-Ethyl-*N′*-(3-dimethylaminopropyl)carbodiimide (EDC), and ethanolamine were supplied by Sigma Aldrich. Unless otherwise specified, all the reagents were prepared using 10 mM PBS in DI water (pH~7.2).

B. Nanocomposite Synthesis

$Ti_3C_2T_x$ MXene nanoflakes were dispersed in DI water using probe sonication for 2 hours, resulting in a 4 mg/ml suspension. In parallel, 50 mg/ml (i.e., 5 wt.%) BSA solution was dissolved in PBS. A mixture containing 5 mg/ml BSA and 0.5 mg/ml MXene was bath sonicated for 30 minutes with a 1-second on/off pulse, followed by heating at 100°C to denature the BSA. The mixture was then centrifuged at 1000 rpm for 15 min to remove excess aggregates and then 1% GA was added (crosslinking ratio 70:1 i.e., 69 µl MXene/BSA mixed with 1 µl 70% GA) to prepare the crosslinked MXene/BSA/GA composite.

C. Sensor Fabrication

The SPCE chip-based nanocomposite-coated IP-10 sensor is shown in Fig. 1. The MXene/BSA/GA composite was drop cast (~5 µl) on the WE of SPCE and left within a wet chamber at room temperature overnight to form the 3D nanostructured hydrogel [7]. Thereafter the chips were washed with PBS with agitation at 400 rpm to remove excess material, followed by drying under a low velocity N_2 stream. The anti-IP-10 antibodies were functionalized on the nanocomposite via Carbodiimide crosslinker chemistry. Briefly, a ternary mixture containing 400 mM EDC, 200 mM NHS, and 50 µg/ml human anti-IP-10 antibody was prepared in 50 mM MES buffer (pH~6.2) and placed on an orbital shaker for 90 min at room temperature to activate functional groups in the antibody. A ~5 µl drop of this mixture was spotted onto the nanocomposite-modified WE, followed by overnight incubation in a wet chamber at room temperature. Thereafter, the GA within the nanocomposite was quenched by 1M ethanolamine for 30 min and 1 wt.% BSA for 1 hr. Each of these fabrication stages included a washing step with ~3 ml PBS followed by drying with N_2. The antibody-functionalized chips were stored at 4°C until further use.

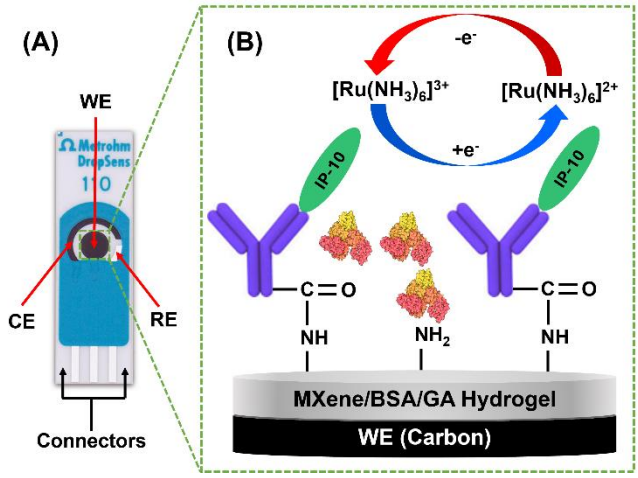

Fig. 1. (A) The screen-printed three electrode chip. (B) Assembly of antibody-functionalized MXene/BSA/GA nanocomposite on the WE. The electrochemical response of antigen-antibody complex formation is quantified via Cyclic Voltammetry-based redox cycling of $[Ru(NH_3)_6]^{2+/3+}$.

D. Material Characterization

Cyclic voltammetry (CV) was performed using the Iviumnstat electrochemical workstation within a potential window of -0.6 to 0.1 V, 10 mV potential steps, and a 100 mV/s scan rate. All the CV responses were measured with a 100 µl drop containing 5 mM $[Ru(NH_3)_6]^{2+/3+}$ in 100 mM KCl in PBS. The extracted currents (µA) were converted to current density (µA/mm^2) using the geometric area of the WE (i.e., 12.56 mm^2). Contact angle (CA) measurements were performed with a ~4 µl droplet placed onto the WE. Each measurement was repeated thrice. The image analysis was performed in MATLAB. UV-VIS spectroscopy of the MXene/BSA/GA nanocomposite was performed in Aquamate 7100 Spectrophotometer

within a wavelength range of 200-800 nm. The surface topography of the SPCEs was mapped using Bruker MultiMode 8-HR atomic force microscope (AFM) in tapping mode. The average (R_a) and root mean squared (R_q) roughness values were measured using NanoScope 2.0 software.

III. RESULTS AND DISCUSSION

A. Cross-linking Mechanism and Wetting Characteristics

GA crosslinks 1° amines in BSA by forming imine bonds, leading to 3D nanostructured porous hydrogel [6]. Previous studies have shown that GA-based crosslinking of BSA occurs via lysine residues present on the surface of BSA. The reaction is characterized by absorbance measurement in the UV-VIS regime as shown in Fig 2. The absorbance was measured before and after the addition of GA, revealing a significant increment in absorbance and peak shift within the 265-280 nm wavelength regime. This difference in the absorbance is attributed to the changes in peptide backbone and protein conjugation during crosslinking [6].

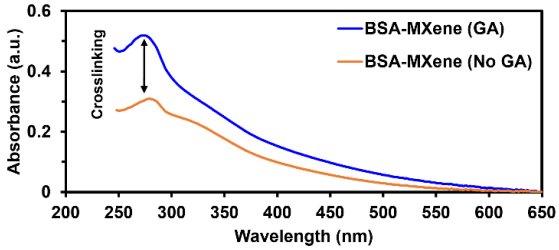

Fig. 2. GA crosslinking of BSA-MXene nanocomposite characterized via UV-VIS spectroscopy. The absorbance peak amplification within the 265-280 nm regime confirms successful crosslinking.

Examination of wetting properties carries essential information on the antibiofouling characteristics of a surface [10]. An ideal EB surface should exhibit reduced susceptibility to non-specific protein adsorption, commonly found in complex biological samples. Non-specific proteins adsorb onto the electrode surface during the sample incubation stage, thus passivating the electrode and hindering the diffusion of electroactive species (e.g., $[Ru(NH_3)_6]^{2+/3+}$) across the electrode-electrolyte interface. The non-specific adsorptions are typically caused by hydrophobic interactions [10], mitigating which is the primary aim of hydrophilic nanocomposite-modified electrodes.

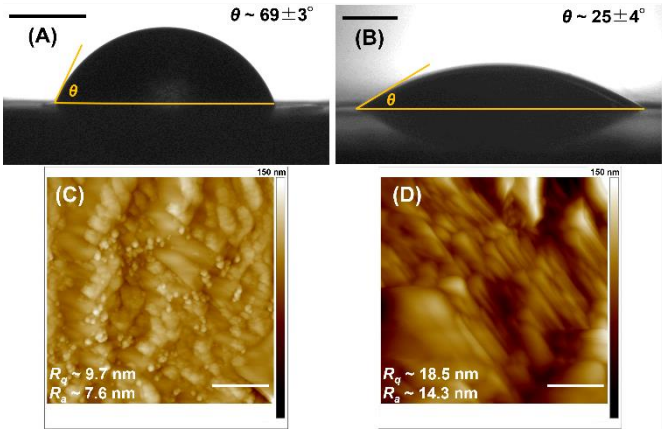

Fig. 3. Static CAs of PBS droplet on (A) bare and (B) nanocomposite coated SPCEs, where scale bars measure 1 mm. The uncertainty is reported based on three replicates. AFM-based surface topography of (C) bare and (D) nanocomposite coated SPCEs. Scale bars represent 500 nm.

Fig. 3 shows the static CA of PBS on the unmodified and nanocomposite-coated SPCEs estimated at 69±3° and 25±4°, respectively. The coating lowers the CA by ~44°, approaching the hydrophilic regime. Electrodes with such high wettability form a hydration layer on the surface and effectively mitigate non-specific protein interactions, thus expected to improve the current response due to specific biomolecule interaction [6]. Further investigation of the AFM images (Figs. 3C and 3D) shows increment in R_a and R_q by reveals ~9 and ~7 nm, signifying the 3D nanocomposite formation the SPCE.

B. Electrochemical Characteristics of Antibody-functionalized Nanocomposite

CV-based redox cycling of $[Ru(NH_3)_6]^{2+/3+}$ was used to quantify the alteration of electron transfer ability across the electrode-electrolyte interface resulted from nanocomposite coating on the SPCE chip and antibody functionalization (Fig. 4). The linear relations between redox peak currents and the square root of scan rate indicate a diffusion-controlled electron transfer process. It is also evidenced that the electroconductive hydrogel coated WE has significantly higher reduction peak current (thus higher sensitivity) compared to the bare WE. This is attributed to: (a) thin layer diffusion enhancement by the 3D porous nanostructure [11] and (b) BSA and MXene both being electronegative act as electron suppliers to the cationic $[Ru(NH_3)_6]^{2+/3+}$ probe. Functionalizing the nanocomposite-modified SPCEs with anti-IP-10 antibody via EDC-NHS covalent coupling lowers the reduction peak current due to a decrease in the electroactive surface area of the nanocomposite.

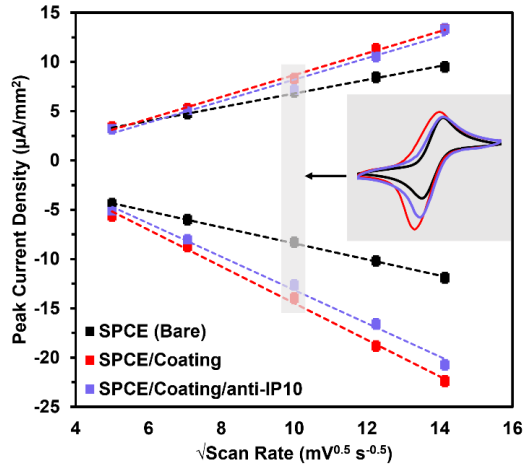

Fig. 4. CV-based oxidation and reduction peak current densities as a function of square root of five different scan rates (25, 50 100, 150, and 200 mV/s) for bare SPCE, after nanocomposite-coating, and after antibody functionalization. The inset shows examples of CV profiles recorded at 100 mV/s scan rate.

C. Sensor Performance

The sensing performance of anti-IP-10 antibody functionalized BSA/GA/MXene coated SPCE chips was investigated by testing various concentrations of IP-10 protein (1-1000 pg/ml) spiked in human serum. The sensing mechanism consists of ~5 µl sample drop casting on the WE followed by incubation at 37°C for 30 minutes and

a washing step with 1 ml PBS. The extent of antigen-antibody complex formation was quantified based on the reduction peak current of $[Ru(NH_3)_6]^{2+/3}$, shown in Fig. 5. The absolute value of the reduction peak current monotonically increased with a higher amount of IP-10 concentration. This indicates a higher amount of antigen-antibody complex formation enhances the electronegativity of the electrode-electrolyte interface, thus easing the reduction mechanism of $[Ru(NH_3)_6]^{3+}$ into $[Ru(NH_3)_6]^{2+}$, and amplifying the peak current. Although the sensor response was found to be linear within the lower range (1-200 pg/ml), the signal saturated at higher concentrations, resulting to a logarithmic response within the 1-1000 pg/ml range. The LOD of the sensor developed was calculated based on the standard deviation of three replicates, resulting in a 3.3 pg/ml IP-10 detection spiked in human serum. The performance of the sensor developed is comparable with commercial ELISA kits linear sensitivity 8-500 pg/ml IP-10 protein [12].

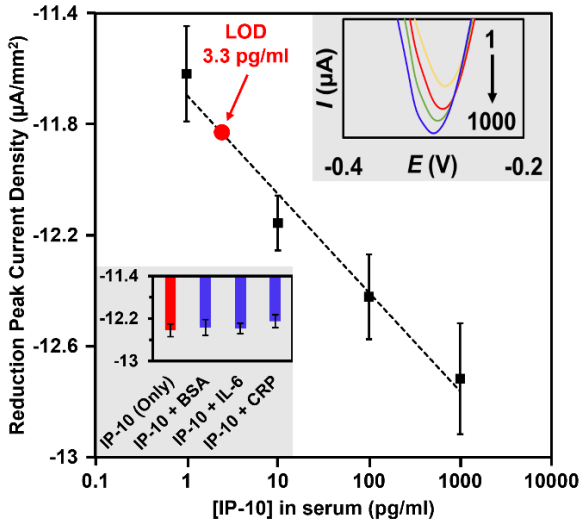

Fig. 5. CV-based reduction peak current densities of antibody functionalized EBs incubated four different concentrations of IP-10 protein (1-1000 pg/ml) spiked in human serum. The *x*-axis if plotted in logarithmic scale. The resultant sensor has an LOD of 3.3 pg/ml. The top inset shows reduction peak current amplification due to a higher amount of protein binding at ~ -0.3 V, while the bottom inset examines selectivity and specificity of the IP-10 sensor against other proteins (e.g., BSA, IL6, and CRP). The span of error bars in each direction is equivalent to the standard deviation of triplicates.

The specificity of the IP-10 sensor was investigated using non-specific proteins such as BSA (10 mg/ml), C-reactive protein (CRP), and Interleukin-6 (100 pg/ml). Each of these proteins was mixed with 100 pg/ml IP-10 protein, which ensured a competitive binding reaction during the sample incubation stage. The specificity tests showed negligible interference from these proteins (blue bars in Fig. 5) when compared to the original response of the 100 pg/ml IP-10 (red bars in Fig. 5), thus proving excellent anti-biofouling characteristic of the nanocomposite. Furthermore, stability tests of the coated SPCEs stored at 4°C over one week showed a <2% change in CV peak currents.

IV. CONCLUSIONS

An SPCE-based EB, coated with MXene/BSA/GA nanocomposite was developed for sensitive and specific detection of IP-10 spiked in human serum, a promising chemokine for monitoring kidney transplant rejection. The sensor has a linear detection range of IP-10 within 1-200 pg/ml with an LOD of 3.3 pg/ml. The label-free sensing protocol offered a single-step detection of IP-10 with a nominal response time of 30 min. UV-VIS characterization confirmed cross-linking characteristics of the hydrogel, while contact angle measurement revealed significant enhancement of the hydrophilicity of the electrode, ultimately reducing non-specific protein adsorption. This could allow for rapid and biofouling-resistant detection of IP-10 in other complex biological matrices, e.g., urine, which can lead to an earlier diagnosis of kidney transplant rejection and individualized treatment protocols.

ACKNOWLEDGMENTS

The work was partially supported by the following grants: Royal Society Newton International Fellowship (NIF\R1\211013) for RG, IHE-Rosetrees grant (UCL-IHE-2020\103), the Wellcome/EPSRC Centre for Interventional and Surgical Sciences (WEISS) (203145Z/16/Z), the InspiringFuture ERC Consolidator fellowship by ERC, UKRI Horizon Europe Guarantee (EP/X023974/1), and Royal Society Wolfson Fellowship.

REFERENCES

[1] Nankivell B J, Chapman J R (2006), "The significance of subclinical rejection and the value of protocol biopsies," *American Journal of Transplantation*, vol: 6(9).

[2] Hirt-Minkowski P, Amico P, Ho J, Gao A, Bestland J, Hopfer H, Steiger J, Dickenmann M, Burkhalter F, Rush D, Nickerson P (2012), "Detection of clinical and subclinical tubulo-interstitial inflammation by the urinary CXCL10 chemokine in a real-life setting," *American Journal of Transplantation*, vol. 12(7), pp.1811-1823.

[3] Van Loon E, Tinel C, de Loor H, Bossuyt X, Callemeyn J, Coemans M, De Vusser K, Sauvaget V, Olivre J, Koshy P, Kuypers D (2023), "Automated Urinary Chemokine Assays for Noninvasive Detection of Kidney Transplant Rejection: A Prospective Cohort Study," *American Journal of Kidney Diseases*, (In Press).

[4] Russo M J, Han M, Desroches P E, Manasa C S, Dennaoui J, Quigley A F, Kapsa R M, Moulton S E, Guijt R M, Greene G W, Silva S M (2021), "Antifouling strategies for electrochemical biosensing: mechanisms and performance toward point of care based diagnostic applications," *ACS sensors*, vol. *6* (4), pp.1482-1507.

[5] Tanak A S, Muthukumar S, krishnan S, Schully K L, Clark D V, Prasad S (2021), "Multiplexed cytokine detection using electrochemical point-of-care sensing device towards rapid sepsis endotyping," *Biosensors and Bioelectronics*, vol. 171, pp. 112726.

[6] Sabaté del Río J, Henry O Y, Jolly P, Ingber D E (2019), "An antifouling coating that enables affinity-based electrochemical biosensing in complex biological fluids," *Nature nanotechnology*, vol. 14 (12), pp. 1143-1149.

[7] Zupančič U, Jolly P, Estrela P, Moschou D, Ingber D E (2021), "Graphene Enabled Low-Noise Surface Chemistry for Multiplexed Sepsis Biomarker Detection in Whole Blood," *Advanced Functional Materials*, vol. 31(16), pp. 2010638.

[8] Timilsina S S, Durr N, Yafia M, Sallum H, Jolly P, Ingber D E (2022), "Ultrarapid method for coating electrochemical sensors with antifouling conductive nanomaterials enables highly sensitive multiplexed detection in whole blood," *Advanced healthcare materials*, vol. 11(8), pp. 2102244.

[9] Kalkal A, Tiwari A, Sharma D, Baghel M K, Kumar P, Pradhan R, Packirisamy G (2023), "Air-brush spray coated Ti_3C_2-MXene-graphene nanohybrid thin film based electrochemical biosensor for cancer biomarker detection," *International Journal of Biological Macromolecules*, vol. 253, pp. 127260.

[10] Wu Q, Hou Q, Wang P, Ding C, Lv S (2023), "Antifouling Electrochemiluminescence Biosensor Based on Bovine Serum Albumin Hydrogel for the Accurate Detection of p53 Gene in Human Serum," *ACS Applied Materials & Interfaces*, vol. 15 (37), pp. 44322-44330.

[11] Jangid K, Gupta R, Sahu R P, Zhitomirsky I, Puri, I K (2022), "Influence of conductive porous electrodes on the apparent electrode kinetics of fenitrothion," *Journal of Electroanalytical Chemistry*, vol. 910, pp. 116200.

[12] Thermo Fisher Scientific, "IP-10 (CXCL10) Human ELISA Kit," *Technical Datasheet, URL: https://www.thermofisher.com/elisa/product/IP-10-CXCL10-Human-ELISA-Kit/KAC2361*